Predeposition Chemistry Underlying the Formation of Germanium Films by CVD of Tetravinylgermane

Philip G. Harrison,* Chantal de Cointet, Djarolla Ograb, and David M. Podesta

Department of Chemistry, Université of Nottingham, University Park, Nottingham NG7 2RD, UK

Pierre Mazerolles

Laboratoire de Chimie Organiques, Universite Paul Sabatier, 118 route de Narbonne, 31077 Toulouse Cedex, France

Roland Morancho and Alex Reynes

Laboratoire des Materiaux en Couches Mences, Ecole Nationale Superieure de Chimie de Toulouse, 118 route de Narbonne, 31077 Toulouse Cedex, France

Received December 6, 1993. Revised Manuscript Received June 13, 1994®

The predeposition chemistry involved in the formation of elemental germanium films by MOCVD using tetravinylgermane as the precursor has been investigated under both static and dynamic conditions. Decomposition of the neat germane under static conditions has been studied using Fourier transform infrared spectroscopy in the temperature range 613–683 K, and is found to be second order with respect to loss of $Ge(CH{=}CH_2)_4$. Second-order rate constants vary from 30.4 l mol^{-1} at 613 K to 128 l mol^{-1} at 683 K, from which Arrhenius analysis yields a value of the activation energy of 186.5 kJ mol^{-1}. Observed products are ethene, ethyne, and butadiene. These data are interpreted in terms of a gas-phase free-radical chain mechanism involving addition of vinyl radicals at the α-carbon of a vinyl group of $Ge(CH{=}CH_2)_4$ followed by elimination of butadiene, and subsequent loss of vinyl radicals from transient $Ge(CH{=}CH_2)_n$ ($n = 1-3$) species. Under dynamic flow conditions using helium as the carrier gas, decomposition of TVG does not commence until ca. 670 K and conversions of >90% are not achieved until ca. 970 K. Under these conditions decomposition is probably an unimolecular process involving successive loss of vinyl radicals from germanium. Ethene, ethyne, and butadiene are again formed together with small amounts of other hydrocarbons. When hydrogen is employed as the carrier gas, the decomposition is more facile and ethene is by far the major hydrocarbon product. The behavior of triethylvinylgermane under flow conditions is similar.

Introduction

During the past few decades the semiconducting properties of germanium films have aroused great interest. Several methods have been employed for the deposition of thin films, including elemental evaporation,[1] cathodic sputtering,[2] glow discharge,[3-5] and MOCVD.[6] Of these, the most versatile is the latter process since the nature of the resulting film can be tailored by appropriate choice of the organogermane precursor molecule.[6] Much attention has been devoted to the nature and properties of the resulting film, but relatively little to the predeposition chemistry of the precursor. This is surprising since it has become apparent that the latter can play an important role in determining the characteristics of the film. In particular, the kinetics and mechanism(s) operating during the pyrolysis process appear to be very important in determining the rate of film deposition and its quality. To establish some general rules concerning the pyrolysis of potential precursor molecules, we have undertaken thermal decomposition studies of several types of organogermanes including simple compounds such as tetraethyl- and tetramethylgermane, tri- and dialkylgermanes, vinylgermanes, allylgermanes, diallylgermacyclopentenes, and 5-germaspiro[4,4]nona-2,7-dienes.[6,7] The goal of this work is not to obtain thin films of pure germanium but to compare the thermal behavior of organogermanes of different structure. In this paper we report a detailed investigation of the gas phase thermal decomposition chemistry of one precursor molecule, tetravinylgermane (TVG), under both static and dynamic flow conditions.

* To whom enquiries should be addressed.

® Abstract published in *Advance ACS Abstracts,* August 15, 1994.

(1) Heavens, O. S. *Proc. Phys. Soc. London* **1952**, *65B*, 788.
(2) Dauvillier, A., *Techn. Rayons X, Paris* **1924**, 21.
(3) Morimoto, A., Kataoka, T.; Kumeda, M.; Shimizu, T. *Philos. Mag. B* **1984**, *50*, 517.
(4) Brodsky, M. H.; Cardona, M.; Cuomo, J. J. *Phys. Rev.* **1977**, *16*, 3556.
(5) Anderson, D. A.; Spear, W. E. *Philos. Mag.* **1976**, *35*, 1.
(6) Mazerolles, P.; Morancho, R.; Reynes, A. *Silicon, Germanium, Tin Lead Compd.* **1986**, *9*, 155.
(7) Avigal, Y.; Itzhak, D.; Schieber, M. *J. Electrochem. Soc.* **1975**, *122*, 1226.

0897-4756/94/2806-1620$04.50/0

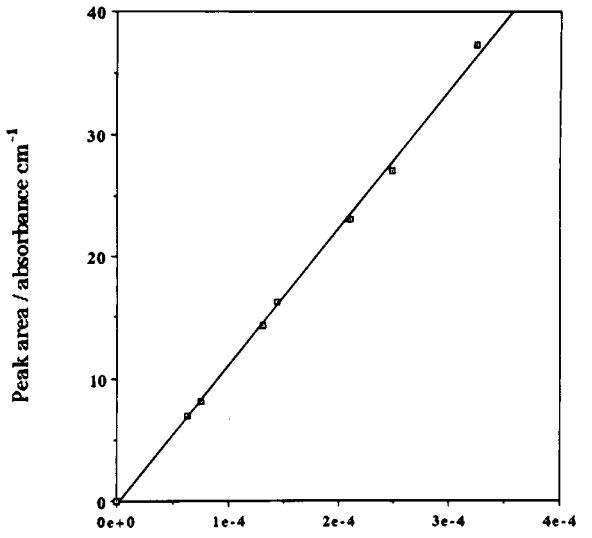

Figure 1. Beer–Lambert plot of absorbance of the ν(Ge–C) band versus pressure for tetravinylgermane (the solid line represents the least-squares fit; value of $R^2 = 0.998$).

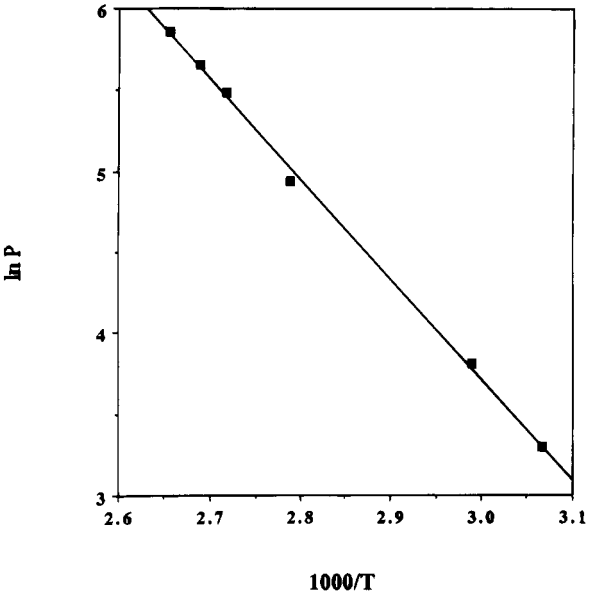

Figure 2. Plot of ln(vapor pressure) versus $10^3/T$ for tetravinylgermane (the solid line represents the least-squares fit; value of $R^2 = 0.999$).

Experimental Section

Tetravinylgermane was prepared by the Grignard method according to literature methods[8] (bp 58–61 °C/45 Torr, lit.[8] 52–54 °C 27 Torr). In the gas phase TVG exhibits infrared bands at 3187, 3061, 3016, 2991, 2956 (ν(CH)), 1905 (2 × 954), 1401 (ν(C=C), 1262, 1004, 960 (δ(CH)), and 598, 550, and 528 (ν(Ge–C)) cm^{-1}. The mass spectrum exhibits fragments due to the parent ion as well as fragments $Ge(CH{=}CH_2)_n^+$ (n = 1–3) resulting from the successive loss of vinyl groups from germanium. Triethylvinylgermane (TEVG) was prepared similarly from triethylchlorogermane.

Infrared Measurements. An infrared cell constructed of Pyrex glass of path length 143.5 mm and diameter 25 mm equipped with CsI windows was used for all the infrared experiments. The cell was connected to a vacuum line system operating at a backing pressure of <10^{-4} Torr. For each experiment, TVG (ca. 5 Torr) was admitted to the cell, which had been preheated to the desired temperature, and spectra recorded at appropriate intervals using a Nicolet Instruments 20SXC spectrophotometer. The cell was kept under isothermal conditions at the desired temperature using a Eurotherm temperature controller. Product identification was by comparison with spectra of authentic samples. Gas phase concentrations of TVG were measured by observing the absorbance changes of the ν(Ge–C) band envelope between 450 and 630 cm^{-1} using the Beer–Lambert plot shown in Figure 1. In the pressure range p = 0–6 Torr, the absorbance/pressure relationship obeys the linear relationship

$$A(\text{Ge–C}) = -0.319 + 6.131p \qquad (R^2 = 0.998)$$

For the cell used in the present study the gas-phase abundance of TVG, C (mol l^{-1}), is therefore given by $C = 1.604 \times 10^{-2}\ p/T$. An initial pressure of 5 Torr at 295 K (corresponding to an abundance of 2.72 × 10^{-4} mol L^{-1}) was employed for all kinetic runs. The variation of vapor pressure, P, with temperature for TVG is shown in Figure 2. The best least-squares fit is given by the equation

$$\ln P = 22.26 - 6.183 \times 10^{-3}/T \qquad (R^2 = 0.999)$$

Flow Studies. The decomposition of TVG under dynamic conditions was carried out in a cold-wall apparatus described previously[6] using either helium or hydrogen as the carrier gas at a flow rate of 10 L min^{-1} passing through a reservoir of TVG at 243 K (corresponding to a concentration of TVG of 2.73 × 10^{-6} mol L^{-1}). The heating zone has a length of 5 cm, and the residence time in the reactor was 0.6 s. Product identification was performed using either gas chromatography or mass spectrometry. Percentage conversions were calculated using the function $[S(0) - S(T)]/S(0)$, where $S(0)$ is the concentration of TVG in the flow mixture prior to reaction and $S(T)$ is the concentration of TVG in the effluent mixture from the CVD reactor at temperature T. Decomposition studies of TEVG were carried out in an identical fashion.

(8) Seyferth, D. *J. Am. Chem. Soc.* **1957**, *79*, 2738.

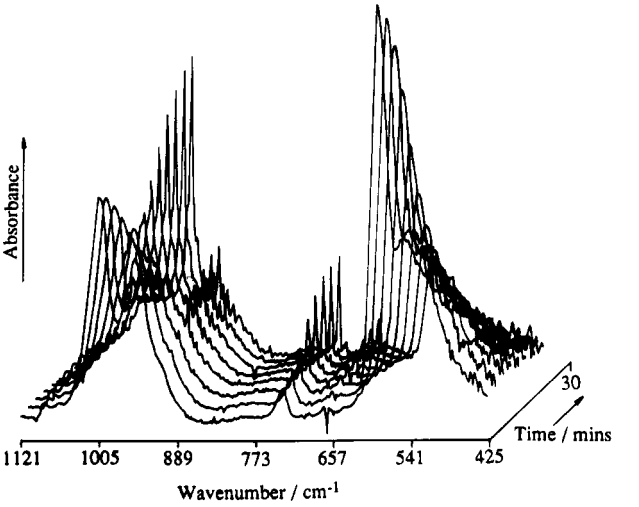

Figure 3. Plot illustrating time-resolved infrared spectra in the range 1120–425 cm^{-1} for the decomposition of tetravinylgermane at 653 K.

Results

Infrared Data. The thermal decomposition of neat TVG at a measurable rate commences at ca. 613 K. During each experimental run the bands characteristic of TVG reduce in intensity, and new bands are observed to grow. A typical series of time-resolved spectra for the decomposition of TVG at 653 K are illustrated in Figure 3, and the initial and final spectra from the

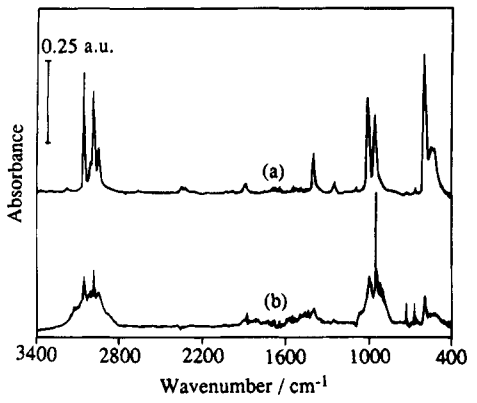

Figure 4. Infrared spectra (3400–400 cm^{-1}) of tetravinylgermane in the gas phase (a) together with that of the final product mixture (b).

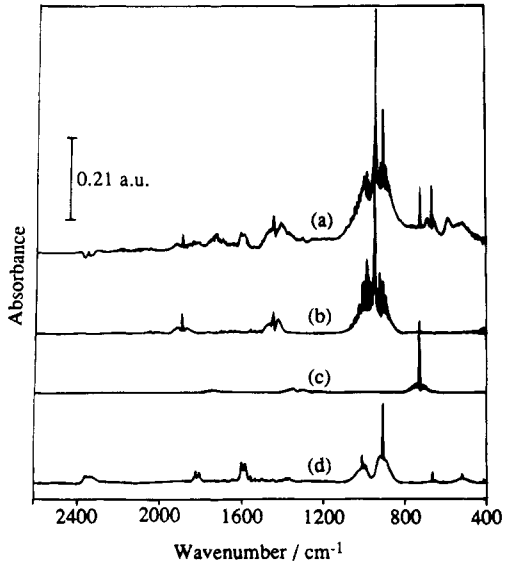

Figure 5. Assignment of constituent components of the reaction mixture: infrared spectra of the product mixture (a) together with spectra of authentic samples of C_2H_4 (b), C_2H_2 (c), and C_4H_6 (d).

reaction are shown in Figure 4. The observed products which are formed during the reaction are ethene, ethyne and butadiene only (Figure 5), and no other hydrocarbon or organogermane species are observed during the course of the reaction.

The decomposition of TVG under the static conditions of the infrared experiments follows second-order kinetics in the range 613–683 K (Figure 6, plots for the two lowest temperatures have been omitted for clarity). The reactions were continued until the peak area of the ν(Ge–C) band envelope had decayed to ca. 20% of its initial value. Absolute values of the second-order rate constants, k, are listed in Table 1, and vary from 0.30 L mol^{-1} at 613 K to 12.8 L mol^{-1} at 683 K. The corresponding Arrhenius plot is linear (Figure 7) and obeys the relationship

$$\ln k = 39.76 - 1.856 \times 102/T$$

from which is derived a value of 185.6 kJ mol^{-1} for the activation energy, E_A.

All three hydrocarbons are produced at the onset of the decomposition of TVG, and their subsequent production proceeds simultaneously in the approximate ratio 10:5:1 for $CH_2{=}CH_2$, $CH_2{=}CHCH{=}CH_2$, and $CH{\equiv}CH$, respectively. That formation of all three products are as a result of the second-order decomposition of TVG is illustrated by the close similarity of the reaction profiles for the cumulative second-order loss of TVG and the cumulative production of the three hydrocarbon products (Figure 8).

Reduction of the initial pressure of TVG resulted in a decrease in reaction rate. Reactions performed in the presence of hydrogen and deuterium gave exactly the same distribution of products as observed for the decomposition of neat TVG, and no deuterium-containing products were observed in the case of the latter. Brief experiments carried out in the presence of methyl iodide (at 643 K) and nitric oxide (at 663 K) as radical initiator and radical inhibitor, respectively, showed that the reaction rate increased by a factor of ca. 4 in the presence of methyl iodide but was retarded by a factor

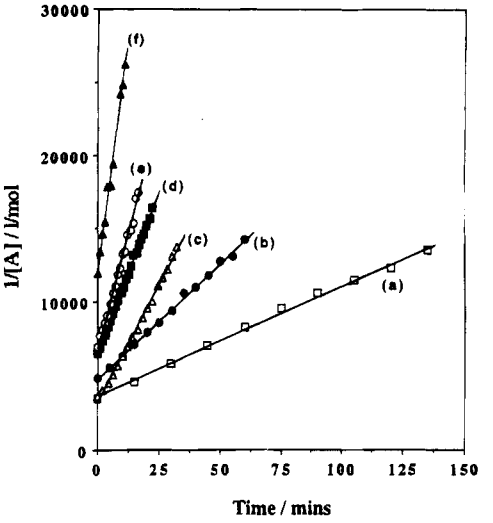

Figure 6. Second-order rate plots for the loss of tetravinylgermane at (a) 633, (b), 643, (c) 653, (d) 663, (e) 673, and (f) 683 K (the solid lines represent least-squares fits; values of $R^2 > 0.99$).

Table 1. Second-Order Rate Constants for the Thermal Decomposition of Tetravinylgermane under Static Conditions

temp/K	second-order rate constant ($\times 10^{-1}$)/L mol^{-1}
613	3.04
623	5.19
633	7.39
643	15.5
653	31.7
663	44.2
673	63.3
683	128

Table 2. First-Order Rate Constants for the Thermal Decomposition of Tetravinylgermane under Dynamic Conditions

temp/K	first-order rate constant ($\times 10^5$)/h^{-1}
673	3.77
723	6.39
773	11.5
823	19.5
873	22.0
923	23.5
973	25.2

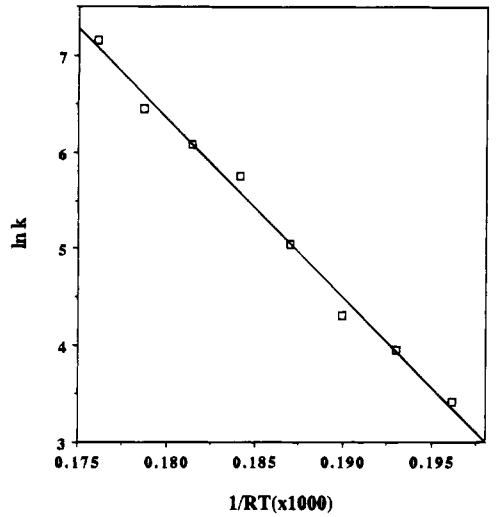

Figure 7. Arrhenius plot for the second-order decomposition of tetravinylgermane in the temperature range 613–683 K (the solid line represents the least-squares fit; value of $R^2 = 0.991$).

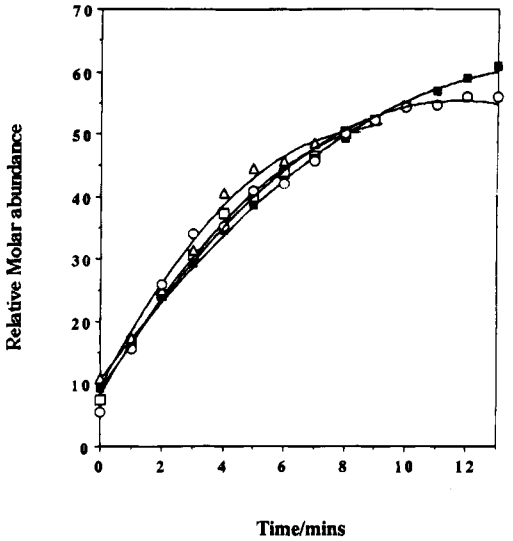

Figure 8. Plot showing the relative distribution of products (○ C_2H_4, △C_4H_6 (×1.93), and □ C_2H_2 (×9.3)) together with the function $\Sigma[(H_2C{=}CH)_4Ge]_2$ (×0.368) for the reaction at 673 K (the solid lines are least-squares binomial fits; values of $R^2 >$ 0.98).

of ca. 6 in the presence of nitric oxide. The addition of ground Pyrex glass to the cell also resulted in an increase in the reaction rate.

Flow Studies. *Tetravinylgermane.* The extent of decomposition of TVG under flow conditions with respect to temperature is illustrated in Figure 9. Decomposition commences at *ca.* 570 K when helium is used as the carrier but at *ca.* 520 K when hydrogen is used as the carrier gas. However, substantial decomposition does not occur until significantly higher temperatures, and 80% conversions are achieved at temperatures of ca. 850 K (H_2) and ca. 900 K (He). Thereafter, the rate of decomposition slows and a maximum conversion of ca. 92% is achieved at a temperature of ca. 1020 K. Products of the decomposition are ethene, ethyne, and butadiene together with smaller amounts of other hydrocarbons including ethane and methane. Figure 10 shows the variation with temperature of the production of the three major hydrocarbon products together with the decomposition of TVG using helium as the carrier gas. As TVG decomposes, ethene and ethyne are

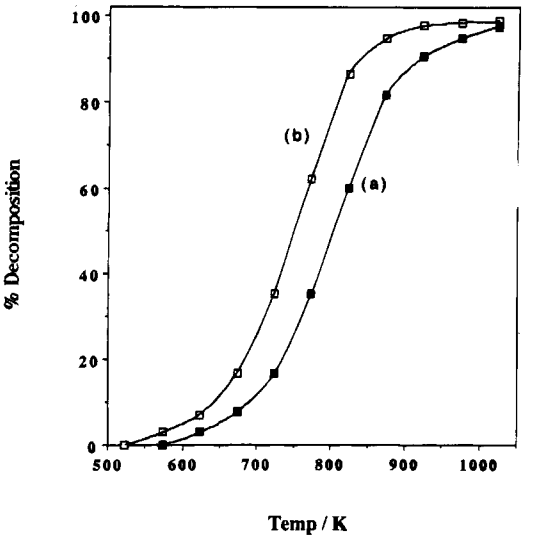

Figure 9. Plot showing the extent of decomposition of tetravinylgermane in the temperature range 523–1023 K under dynamic conditions using (a) helium and (b) hydrogen as the carrier gas.

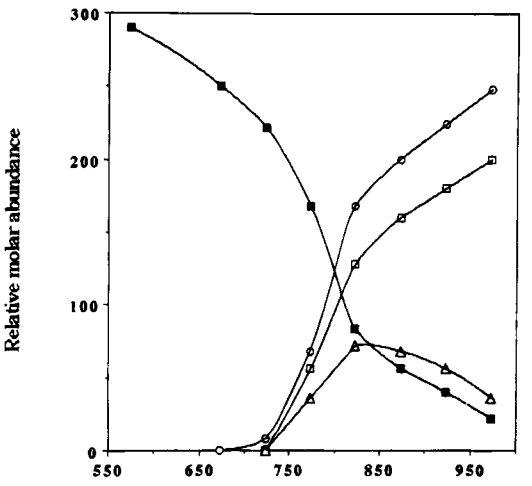

Figure 10. Plot showing the loss of tetravinylgermane (■) and the formation of C_2H_4 (○) (×4), C_4H_6 (×4) (△), and C_2H_2 (×4) (□) under dynamic conditions in the temperature range 550–1000 K.

produced in similar amounts which increase with temperature. The amount of butadiene is, however, significantly lower than the other two components and increases to a maximum level at ca. 770 K decreasing thereafter. At 1020 K the proportion of butadiene in the mixture is very low.

The composition of the hydrocarbon product mixture is substantially different depending upon whether helium or hydrogen is used as the carrier gas. Figure 11 illustrates the variation in the percentage composition of the product mixtures with temperature in the two cases. With helium as the carrier gas, although ethene is the major component, both ethyne and butadiene are formed in large quantities. Other components constitute 1–2% of the mixture but do not appear at temperatures below 823 K. Using hydrogen as the carrier gas the proportion of both ethyne and butadiene are substantially reduced compared to the levels when helium is the carrier gas. The proportions of both rise to a maximum at temperatures around 873 K decreas-

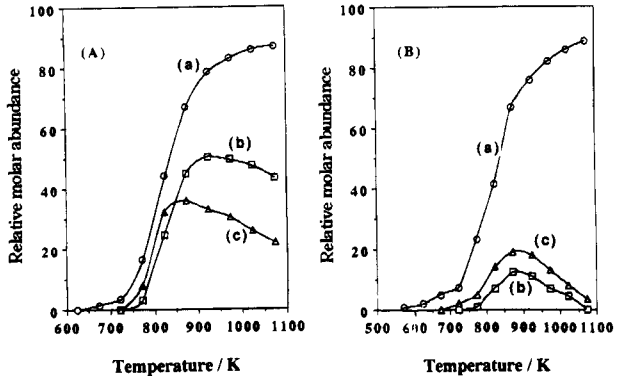

Figure 11. Plot showing the relative amounts of C_2H_4 (a), C_2H_2 (b), and C_4H_6 (c) under dynamic conditions using (A) helium and (B) hydrogen as the carrier gas in the temperature range 550–1000 K.

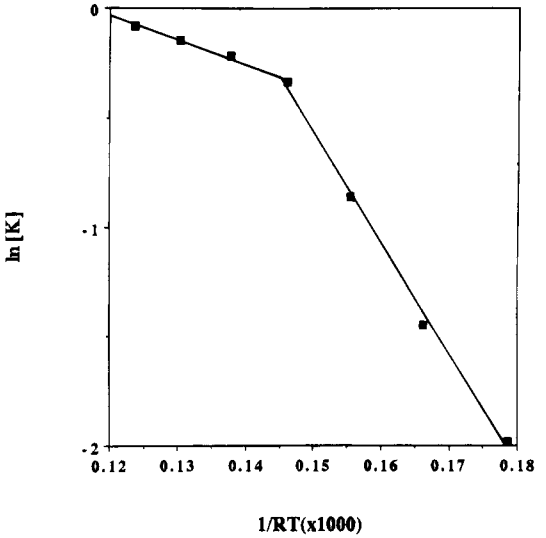

Figure 12. Arrhenius plot for the decomposition of tetravinylgermane in the temperature range 550–1000 K (the solid lines represent least-squares fits; values of $R^2 > 0.99$).

ing thereafter, and at a temperature of ca. 1070 K these two components are essentially absent from the product mixture. However, other hydrocarbon constituents including methane and ethane are formed even at the lowest temperature studied (623 K) and rise steadily as the decomposition progresses forming a total of 15% at 1070 K.

The Arrhenius plot derived from the flow data for the decomposition of TVG using helium as the carrier gas is shown in Figure 12. The plot comprises two distinct linear parts indicating the occurrence of two distinct mechanistic regimes. In the temperature range 673–823 K the activation energy is determined to be 50.7 kJ mol^{-1} while in the range 823–973 K the activation energy is substantially smaller at 11.3 kJ mol^{-1}.

Triethylvinylgermane. The behavior of TEVG under flow conditions is quite similar to that exhibited by TVG (Figure 13). The onset of decomposition using helium as the carrier gas occurs at temperatures >573 K, reaching 60% decomposition at 873 K and 92% decomposition at 973 K. The major product over the whole temperature range is ethene with only small quantities of ethyne and butadiene being produced. Triethylgermane is also formed in small amounts at temperatures of 823 K and above.

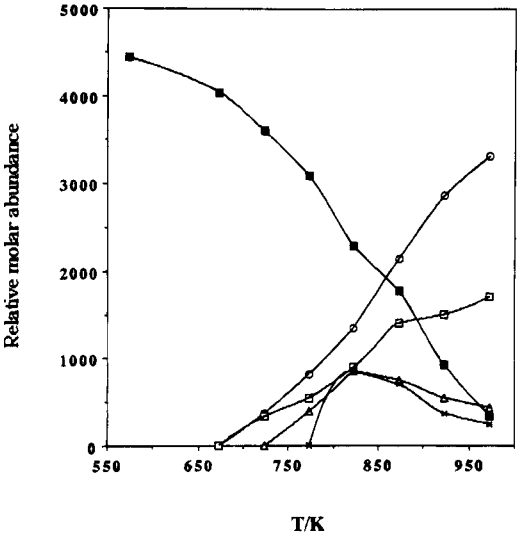

Figure 13. Plot showing the loss of triethylvinylgermane (/2.5) (■) and the formation of C_2H_4 (○), C_4H_6 (×50) (△), C_2H_2 (×50) (□), and $(C_2H)_3Ge_3H$ (×50) (×) under dynamic conditions in the temperature range 550–1000 K.

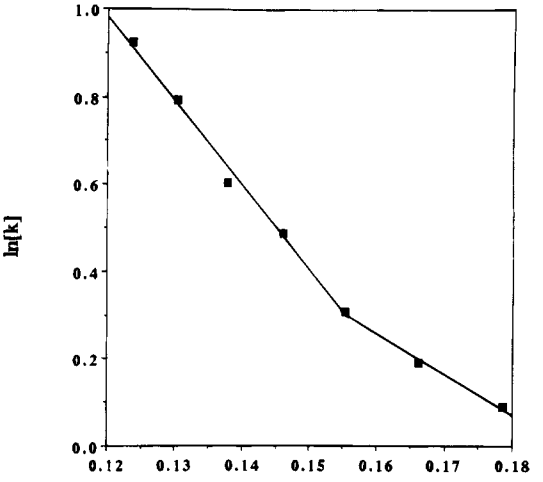

Figure 14. Arrhenius plot for the decomposition of triethylvinylgermane in the temperature range 550–1000 K (the solid lines represent least-squares fits; values of $R^2 > 0.99$).

The Arrhenius behavior exhibited by TEVG (Figure 14) is also similar to that shown by TVG showing a discontiuity at 773 K. Below this temperature the activation energy is 9.3 kJ mol^{-1} while in the range 773–973 K the activation energy is 19.2 kJ mol^{-1}.

Discussion

Detailed studies of the thermal decomposition of a number of organogermane compounds including $GeMe_4$[7,9] $GeEt_4$,[7,10] and $GeMe_3H$[11] have been reported. A preliminary study of the decomposition of TVG showed the products to be ethene, ethyne, butadiene, and hydrogen,[12] while a flash pyrolysis study of $Sn(CH{=}CH_2)_4$ has shown that similar products (ethyne 52%, ethene 36%,

(9) Taylor, J. E.; Milazzo, T. S. *J. Phys. Chem.* **1978**, *82*, 847.
(10) Geddes, R. I.; Mack Jr., E. *J. Am. Chem. Soc.* **1930**, *53*, 4372.
(11) Harrison, P. G.; McManus, J.; Podesta, D. M. *J. Chem. Soc., Chem. Commun.* **1992**, 291.
(12) Sefiani, J. Thèse, 3° Cycle, I.N.P.T., 1986.

H_2 8%, and butadiene 3%) are also obtained in that case.[13]

In the present study the decomposition of TVG under both static and dynamic conditions may be represented by the overall equation

$$Ge(CH{=}CH_2)_4 \rightarrow GeC_x + CH_2{=}CH_2 + CH{\equiv}CH + CH_2{=}CHCH{=}CH_2$$

in which the major gaseous products are the hydrocarbons ethene, ethyne, and butadiene, and the germanium is deposited as a carbon-containing film. However, because of the different conditions, quite different mechanisms operate in the two cases. Under static conditions the gas-phase abundance of TVG is relatively high and the collision probability between the molecules and the wall is high because the residence time is long. In contrast, under the dynamic flow conditions used in the MOCVD experiments (cold-wall reactor), the residence time is short and the wall effect is minimized.

That the process involves radicals is corroborated by the observed enhancement of reaction rate when the decomposition under static conditions is carried out in the presence of methyl iodide and its retardation in the presence of the radical scavenger nitric oxide. The observed second-order nature with respect to TVG is corroborated by the observed decrease in rate with decreasing initial pressure of TVG. These observations are rationalised by the radical chain process shown in Scheme 1 involving initiation, propagation, and termination steps. Homolytic metal–carbon bond dissociation such as that proposed in (1) is well characterized for many organometallic systems and leads to an initial source of vinyl radicals. There are no examples of H-atom abstraction by radicals from unsaturated systems. Rather, the addition of radicals to carbon–carbon multiple bonds is well established. In particular, a variety of radicals Q• including PhS•, PhSe•, $PhSO_2$•, $(EtO)_2P(O)$•, and $c\text{-}C_6H_{11}$• have been shown to react with vinyltributylstannanes via the addition–elimination process shown in Scheme 2.[14,15] Hence we favor radical addition (2) followed by radical elimination (3)[16] for the two propagation steps in the process. The trivinylgermyl radical thus generated undergoes facile loss of vinyl radicals to give ultimately a deposited germanium film. Termination will be by the self-reaction of vinyl radicals giving ethene and ethyne (8) or butadiene (9). The self-reaction of trivinylgermyl radicals to give hexavinyldigermane as a termination step can be excluded since no hexavinyldigermane is formed. Recombination of vinyl and trivinylgermyl radicals is possible but would not be detected in the present study. The effect of this would, however, only be on the absolute values of the observed rate constants.

(13) Christianson, M.; Price, D.; Whitehead, R. *J. Organomet. Chem.* **1975**, *102*, 273.
(14) Russell, G. A.; Ngoviwatchai, P. *Tetrahedron Lett.* **1986**, *30*, 3479.
(15) Russell, G. A.; Ngoviwatchai, P.; Tashtovsh, H.; Hersberger, J. *Organometallics* **1987**, *6*, 1414.
(16) The reverse of this reaction, i.e.

$$\dot{G}e(CH{=}CH_2)_3 + CH_2{=}CH\text{-}CH{=}CH_2 \xrightarrow{k_{-3}} [\dot{C}H_2CH(CH{=}CH_2)]Ge(CH{=}CH_2)_3$$

may also occur, the effect of which would be to modify the apparent value of k_3.

Scheme 1

Initiation

$$Ge(CH{=}CH_2)_4 \xrightarrow[\text{wall}]{k_1} \dot{G}e(CH{=}CH_2)_3 + \dot{C}H{=}CH_2 \quad (1)$$

$$2Ge(CH{=}CH_2)_4 \xrightarrow{k_{1'}} Ge(CH{=}CH)_4{}^* \; \dot{G}e(CH{=}CH_2)_3 + \dot{C}H{=}CH_2 \quad (1')$$

Propagation

$$Ge(CH{=}CH_2)_4 + \dot{C}H{=}CH_2 \xrightarrow{k_2} [\dot{C}H_2\text{-}CH(CH{=}CH_2)]Ge(CH{=}CH_2)_3 \quad (2)$$

$$[\dot{C}H_2CH(CH{=}CH_2)]Ge(CH{=}CH_2)_3 \xrightarrow{k_3} H_2C{=}CHCH{=}CH_2 + \dot{G}e(CH{=}CH_2)_3 \quad (3)$$

$$\dot{G}e(CH{=}CH_2)_3 \xrightarrow{k_4} Ge(CH{=}CH_2)_2 + \dot{C}H{=}CH_2 \quad (4)$$

$$Ge(CH{=}CH_2)_2 \xrightarrow{k_5} GeCH{=}CH_2 + \dot{C}H{=}CH_2 \quad (5)$$

$$Ge(CH{=}CH_2)_2 \xrightarrow{k_6} Ge + CH_2{=}CHCH{=}CH_2 \quad (6)$$

$$GeCH{=}CH_2 \xrightarrow{k_7} Ge + \dot{C}H{=}CH_2 \quad (7)$$

Termination

$$2\dot{C}H{=}CH_2 \xrightarrow{k_8} H_2C{=}CH_2 + HC{\equiv}CH \quad (8)$$

$$2\dot{C}H{=}CH_2 \xrightarrow{k_9} H_2C{=}CHCH{=}CH_2 \quad (9)$$

$$2\dot{G}e(CH{=}CH_2)_3 \rightarrow Ge_2(CH{=}CH_2)_6 \quad (10)$$

Scheme 2

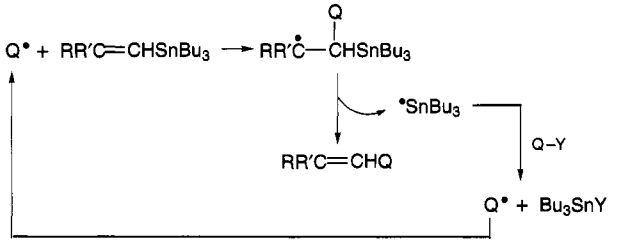

Assuming steady-state conditions, this reaction scheme leads to the kinetic rate equation

$$-\mathrm{d}/\mathrm{d}t\,[Ge(CH{=}CH_2)_4] = \frac{k_2{}^2}{(k_8+k_9)}\frac{2k_5}{(k_5+k_6)}[Ge(CH{=}CH_2)_4]^2$$

fully consistent with the observed second-order kinetic data for the loss of TVG. This derived rate equation

Scheme 3

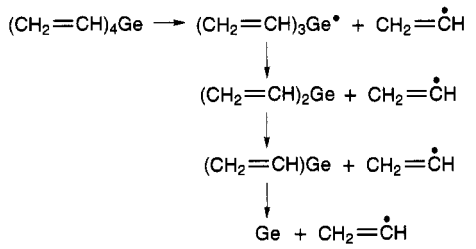

indicates that the activation energy, E_A, is a composite involving the five process (2), (5), (6), (8), and (9), which would predict an activation energy for the overall reaction of

$$E_A = 2E(2) + E(5) - \overline{\{E(8) + E(9)\}} - \overline{\{E(5) + E(6)\}}$$

where the two latter terms are the weighted means of the values inside the brackets. Since radical self-combination generally occurs with very small or zero activation energy, the terms $E(8)$ and $E(9)$ are expected to be ≈ 0. The values of $E(5)$ and $E(6)$ are also expected to be similar, and hence the value of $[E(5) - \{E(5) + E(6)\}]$ will also be ≈ 0 or very low. Thus, the activation energy, E_A, approximates to $2E(2)$, i.e., E_A is an estimate of twice the energy of activation for the addition of vinyl radicals to TVG. Thus, the value of $E(2)$ is determined to be 93 kJ mol^{-1}.

Under the very dilute conditions of the flow experiments, decomposition is not initiated until ca. 673 K, whereas under static conditions where the level of TVG is 100-fold higher initiates at a much lower temperature (613 K). Although the product distribution is similar, it is apparent that mechanistically two different reaction pathways are operating in the two cases. The conditions of the flow experiment serve to preclude a bimolecular process as in Scheme 1, and a unimolecular process similar to that proposed previously for the pyrolysis of tetramethyl- and tetraethylgermane[7,9,10] involving the successive loss of vinyl radicals from germanium (Scheme 3) is proposed. The observed hydrocarbon products will be formed by subsequent reactions of the vinyl radicals. The unimolecular decomposition does not commence until temperatures >673 K, whereas in the static experiment decomposition occurs at much lower temperatures, indicating tht a simple unimolecular homolytic bond-dissociation step is not likely for the initiation step which is either bimolecular (1′) in nature or is promoted by a "wall" effect (1) or both.

Under both static and flow conditions ethene is the major product, with ethyne and butadiene being formed in lower amounts. The primary source of these hydrocarbons is by vinyl radical combination, but at higher temperatures secondary reactions may occur. Pease[17] has shown that above 800 K decomposition of ethene leads to the formation of ethane, methane, and H_2, while below that temperature the products contain butene. Kordysh[18] has observed that ethyne is essentially stable at temperatures <ca. 773 K, but Ogura[19] has demonstrated that above 1100 K pyrolysis occurs to give primarily $CH_2{=}CHC{\equiv}CH$, $CH_2{=}CHCH{=}CH_2$, and H_2. Butadiene begins to decompose at 823 K,[12,20] and in the range 1113–1153 K Kopinke[21] has shown that several products including ethene, methane, cyclopentadiene, and ethyne are formed. Thus, especially at high temperatures, the composition of the hydrocarbon product mixture may be quite complex.

Scheme 4

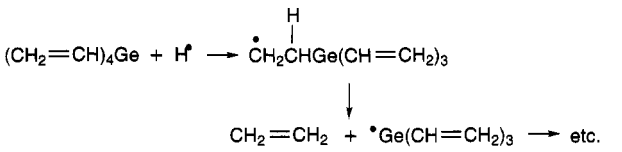

When hydrogen is used as the carrier gas, the decomposition is more facile and ethene is by far the major hydrocarbon product suggesting that hydrogen is participating in the decomposition process. The $H_2 \rightarrow 2H^\bullet$ dissociation is significant to any extent only at ca. 2000 K but is known to be catalyzed by metals such as Ir, Pd, and Pt,[22] and it is possible that catalytic dissociation may also occur in the present case. Further, H$^\bullet$ radicals are known to add efficiently to alkenes such as ethene.[23] We, therefore, suggest that the promoting effect of hydrogen is by the participation of H$^\bullet$ radicals as illustrated in Scheme 4. Additionally, an alternative mode of participation of H_2 has been suggested by Avigal[7] in which organic radicals R$^\bullet$ abstract hydrogen forming RH and generating an H$^\bullet$ radical. That no deuterium-containing products are formed in the static infrared experiments is because these were carried out at a significantly lower temperature than those performed in the MOCVD reactor.

The behavior of TEVG under flow conditions is similar to that of TVG. The major product over the whole temperature range is ethene with small quantities of ethyne, butadiene, and triethylgermane, and a similar mechanism involving organogermyl, ethyl, and vinyl radicals may be formulated. The formation of triethylgermane is interesting and corroborates the intermediates formation of $Et_3Ge^\bullet$ which can abstract hydrogen most probably from another molecule of TEVG.

Conclusions

These data indicate that different mechanisms operate under the two experimental conditions used. Under static conditions using relatively high pressures of TVG a free-radical chain process operates with a rate which is second order in loss of TVG with onset of reaction occurring at ca. 613 K. Under dynamic flow conditions with a concentration of TVG 2 orders of magnitude lower using helium as the carrier gas, decomposition does not occur until ca. 670 K with first-order loss of TVG by a radical process. Use of hydrogen as the carrier gas facilitates the decomposition. The major products under both static and dynamic conditions are ethene, ethyne, and butadiene.

(17) Pease, R. N. *J. Am. Chem. Soc.* **1930**, *52*, 1158.
(18) Kordysh, E. I.; Glikin, M. A.; Kovalivnich, A. M.; Raikova, N. S.; Lakhmanchuk, L. S. *Khim. Tekhnol. (Kiev)* **1976**, *23*; *Chem. Abstr.* **1977**, *86*, 123702p.
(19) Ogura, H. *Bull. Chem. Soc. Jpn.* **1977**, *50*, 1044.
(20) Gerault, P. Thèse, 3° cycle, I.N.P.T., 1981.
(21) Kopinke, F. D.; Ondruschka, B.; Zimmermann, G. *Tetrahedron Lett.* **1983**, *24*, 869.
(22) Mackay, K. M. In *Comp. Inorg. Chem.* **1973**, *1*, 16.
(23) Westenberg, A. A.; de Haas, N. *J. Chem. Phys.* **1969**, *50*, 707.